



INTERNATIONAL ATOMIC ENERGY AGENCY
UNITED NATIONS EDUCATIONAL, SCIENTIFIC AND CULTURAL ORGANIZATION



INTERNATIONAL CENTRE FOR THEORETICAL PHYSICS
34100 TRIESTE (ITALY) · P.O. B. 586 · MIRAMARE · STRADA COSTIERA 11 · TELEPHONE: 9360-1
CABLE: CENTRATOM · TELEX 460891-1

H4.SMR/303 -17

**WORKSHOP
GLOBAL GEOPHYSICAL INFORMATICS WITH APPLICATIONS TO
RESEARCH IN EARTHQUAKE PREDICTIONS AND REDUCTION OF
SEISMIC RISK**

(15 November - 16 December 1988)

**A TIME DEPENDENT MODEL OF
SEISMICITY FOR A SUBDUCTION ZONE**

A.M. GABRIELOV

**Institute for Physics of the Earth
Academy of Sciences of the USSR
10 Bolshaya Gruzinskaya
Moscow D242, USSR**

&

Q. LI, N. NAZER & E. NYLAND

**University of Alberta
Dept. of Physics
Edmonton T6G 2J1
Canada**

A Time Dependent Model of Seismicity for a Subduction Zone

A.M.Gabrielov
Institute for Physics of the Earth
Academy of Sciences of the USSR
10 Bolshaya Gruzinskaya, Moscow D242, USSR

Q. Li, N. Nazer, and E. Nyland
Department of Physics, University of Alberta
Edmonton, Canada T6G 2J1

Preliminary and Subject to Revision

Abstract

Introduction

The seismicity on the Vancouver Island area is concentrated on the Pacific North American plate boundary, where the Pacific plate fragments into the Explorer and the Juan de Fuca Plate which then subduct under the North American plate. It includes the lithospheric seismicity associated with the transition from the Pacific into the North American plate. The three strongest main shocks of magnitudes above 6.0 that occurred recently in the subduction of Explorer and Juan de Fuca plates were preceded by activation of the earthquake flow in the lower magnitude range both in space and time. The time and space pattern of those strong earthquakes were analyzed (Brown et al. 1988) by pattern recognition algorithm M8. This study used the number of main shocks, the ratio of average radius of a fracture to the average event separation, the deviation of the rate of main shocks from its long term linear trend and the bursts of seismicity. All strong earthquakes were preceded by a high level of foreshocks, a high ratio of fracture radius to event separation and bursts of seismicity. The strong event of April 29, 1965 at 47.4N, 122.3W was also preceded by the high deviation of the rate of main shocks from the long term linear trend. The strong event of December 20, at 49.0N, 128.7W shows the activation quiescence scenario. After about four years quiescence, the strong earthquake occurred at the boundary of the activated area.

The observation that recognizable patterns precede large earthquakes in the Vancouver Island area, and that these patterns are similar to those observed elsewhere with the M8 algorithm (Keilis-Borok and Kosobokov 1984) suggests that models of the seismic generating mechanism might be possible. Since there is generally not enough data to justify strictly empirical earthquake predictions such models might assist in the problem of predicting strong earthquakes in this area. The construction of a physical model for earthquake mechanism and its use to generate the entire earthquake cycle has been approached experimentally (Burridge and Knopoff 1967), kinematically (Savage and Prescott 1978; Spence and Turcotte 1979; and Savage 1983) and dynamically (Dieterich 1978, 1979; Rice 1983; Rice and Tse 1986; Stuart 1985, 1986; Rundle 1987).

The mass-spring model (Burridge and Knopoff 1967) was too simple to account for the complexity of a real fault system. With a constitutive relation for the fault zone material we can exploit the idea that instead of an abrupt drop of stress from the static to the dynamic value with the onset of slip, there is a transition caused by a decrease of fault strength from peak to residual value. Such an instability is then interpreted as an earthquake (Rice 1979). This is valid, for slip weakening has been observed in laboratory shear tests. A rate dependence of friction also exists and an important feature of both the slip weakening and rate dependence relation is the appearance of a characteristic sliding distance in the equations describing the system. Rundle (1987) represents earthquakes as a fluctuation about the long term motion of a plate. He describes the physics of earthquake occurrence in terms of a functional potential for the external stress on the fault plane. The model shows the transition from a spatially ordered, temporally disordered state to a spatially disordered, temporally ordered state, and for long enough faults, the dynamics are chaotic.

A simple model designed specifically to support attempts at earthquake prediction (Gabrielov et al. 1986) exploits the hierarchical block structure of the lithosphere (Sadovsky ???). In this hierarchical structure blocks of the lithosphere are connected by thin, weak, less consolidated boundary layers, such as transition zones, lineaments, or tectonic faults. In the seismo-tectonic process major deformation and most earthquakes occur in such boundary layers. The boundary layers themselves have block structure and are systems of blocks of lesser scale. In Gabrielov's model a seismic region is represented as a system of absolutely rigid blocks divided by infinitely thin, elastic boundary layers. The system of

blocks moves because the motion of the boundary blocks is prescribed but relative displacement of all blocks much smaller than their characteristic dimension. As the blocks are rigid, all deformation takes place in the boundary layers and the corresponding stresses depend on the value of relative displacement of blocks. This dependence is assumed linear elastic up to a strength threshold when a boundary layer breaks, stress drops, and an earthquake is said to occur.

Different time scales are an essential property of the model and in the extension discussed below these different time scales lead to a stiff system of differential equations. The boundary blocks move with a constant rate in "slow", or tectonic time. The slowness of this time means that the whole system of blocks is in a quasistatic equilibrium state in which the sum of all the forces and moments acting on each block is zero. After a break the system of blocks in the model moves toward a new equilibrium state by means of processes which must be described on a much shorter time scale than that used to describe tectonic deformation. From the point of view of this time scale, which we call "fast time", the position of the boundary blocks which move at a much lower rate in "slow time" is unchanged during the transition to a new equilibrium point. It is central to this approach that processes of very different time rates dominate at different instants during the evolution of the system. When the system reaches a new equilibrium state elastic interaction and strength are restored and the rapid processes are turned off. This healing, which means strength exists across the faults that developed is necessary to ensure the process is stationary. As time evolves an artificial catalog of earthquakes in which each event is characterized by its time of occurrence, source or the pattern of breaks, and magnitude defined as the logarithm of the energy released by the system of blocks between the old and the new equilibrium states is generated.

An important assumption is contained in the statement that boundary blocks move at a constant rate and that earthquakes occur under essentially constant displacement boundary conditions. The model assumes that the stresses that drive plates do not directly affect seismo-tectonic zones but rather that the seismo-tectonic zones are controlled by the constant motion generated by these plate driving stresses. If we drop this assumption and treat the model as having constant stress boundary conditions earthquake ruptures in the model would never reach equilibrium.

The modeling discussed in this paper is a development on this approach. A time dependent finite element model permits relative motion between some of the elements. This relative motion is controlled by viscous shearing in a fault zone whose rheology is intrinsically non-linear and considers the temperature dependence of apparent viscosity explicitly. The model can be reduced to a system of ordinary differential equations that describe the fault motion in the elastic matrix of the surrounding rock. Solution of these equations indicates time intervals of rapid motion which we identify with earthquakes. The matrix around the visco-elastic fault zone is modeled by elastic, constant strain triangular elements. Since the width of a fault is much smaller than the scale of such a tectonic block, we ignore the thickness of the fault zone and model each fault with a number of infinitely thin interface elements.

The elastic moduli of these interface elements were taken as the ratio of the elastic modulus of the fault zone material and the fault zone thickness. On a real fault zone the relative displacement is of the same order as that of two points with the separation of tectonic block scale and not on a fault zone. Therefore in our finite element model we chose the elastic modulus for the fault zone so that the relative displacement of the nodes on two surfaces of the fault should be of the same order as the relative displacement of off-fault nodes. We chose the Poisson ratio of an interface element close to 0.5 in order to make the compressibility of the fault zone material much larger than the shear modulus.

Models with elastic elements and temperature dependent fault rheology

The material in fault zones is rock and at temperatures $T > T_m/3$, where T_m is the absolute melting temperature, and for long duration of application of stress the creep rate in most rock depends on temperature and pressure by

$$\dot{\epsilon} = D_0 f(\tau) e^{\frac{AT_m}{T}} \quad (1)$$

(Weertman 1970). D_0 and A are material parameters, ϵ is the shearing strain and $f(\tau)$ is a function of shearing stress or deviatoric stress τ . Since T_m varies with pressure, this relation is also pressure dependent. At low shearing stresses $f(\tau)$ is a linear function of τ , a specific atomic model of which could be the diffusive process known as Nabarro-Herring or Coble Creep. At higher stresses where solidus creep is more readily measurable $f(\tau)$ is a non-linear function of τ generally taken as a power law of the form τ^n , with n in the range of 2 to 5. When $\tau > 10^{-3}\mu$, where μ is modulus of quasi rigidity governing rapid deformation of material, (Weertman and Weertman 1975), the power law breaks down and a more rapidly varying function of τ has to be considered. At such a high shearing stress, an exponential dependence of $f(\tau)$ has been suggested (Dorn 1955, Van Bueren 1961, and others). A constitutive equation that represents these different regimes of stress dependence below T_m and at the same time has some physical basis may be written as

$$\dot{\epsilon} = c_0^{-1} e^{\frac{E}{kT}} \sinh \frac{v\tau}{kT} \quad (2)$$

where v and c_0 are parameters, E is an activation energy, k is Boltzmann's constant, and T is absolute temperature. A general physical basis for the form of equation (2) can be given in terms of thermally activated dislocation movement that becomes biased in a particular direction by the applied shear stress (Van Bueren 1961, Feltham 1966).

If the stress τ is constant the temperature profile in this system, which evolves in a quasi-static way, can be found as a solution of the conductive heat transfer equation with distributed heat sources per unit volume.

$$\rho c_p \frac{\partial T}{\partial t} - K \frac{\partial^2 T}{\partial x^2} = \tau \dot{\epsilon} = \text{distribution of heat} \quad (3)$$

where ρ is density, c_p is specific heat, K is conductivity, T is temperature, x is direction of heat flow, and t is time. If this temperature dependent viscous shear occurs on a thin layer of thickness $2a$ equations 2 and 3 can be approximated in a useful way. Let T be the temperature at the center of the layer and T_0

be the temperature of the surrounding medium. Equation 3 becomes $\rho c_p \frac{dT}{dt} = \tau \dot{\epsilon} - 2 \frac{K}{a} (T - T_0)$ and if the

anelastic displacement at $\pm a$ is $\pm \Delta$ the shear strain rate $\dot{\epsilon} = \frac{1}{2a} \frac{d\Delta}{dt}$. Defining σ as the mass per unit area of

this fault, and $K_1 = 4K/a$ as the conductivity for thin fault we have $\sigma c_p \frac{dT}{dt} = \tau \frac{d\Delta}{dt} - K_1 (T - T_0)$. The time rate of change of anelastic displacement can be written in terms of the stress and the temperature by

writing 2 as $\frac{d\Delta}{dt} = \frac{a}{c_0} e^{\frac{-E}{kT}} \sinh \frac{vT}{kT}$ and the temperature dependent, creep behaviour of a thin, uniform, fault element can be fully defined by

$$\frac{d\Delta}{dt} = A \tau \frac{d\Delta}{dt} - B (T - T_0)$$

This development assumes that inertial effects are negligible and that stress is constant over the thickness $2a$ of the fault element. If either condition is violated we can say we have an instability which

can be interpreted as a seismic event. Inertial effects clearly become important when $\rho \dot{v} = \frac{\tau}{a}$ where \dot{v} is rate of change of strain rate integrated with respect to x from $-a$ to a . Let μ be the shear elastic modulus of

the fault material. If the creep properties of the medium change significantly in times of the order $\sqrt{\frac{2a}{\mu}}$

inertial effects must be included and in this case we perceive a rupture to be occurring.

Finite Element Models with Fault Elements

The finite element problem for a model with discontinuities can be formulated as the solution of

$$Kd = f + A_1 b + A_2 \delta + A_3 g$$

where K is a stiffness matrix, d is the vector of N nodal displacements, and the source terms are contributions from boundary displacements b , anelastic fault displacements δ , and gravity g respectively. The matrices A_1 , A_2 , and A_3 are the transformations that convert their respective vectors into source terms or body force equivalents and A_2 contains the effective shear modulus of the fault. In the actual process of computation the terms on the right hand side arise from constraints such as boundary constraints, slips computed on fault elements by methods external to the elastic finite element calculation, and initial conditions. For fault zone dynamics the shear stress on the M fault elements is $\tau = M_1 d + M_2 \Delta$ and

$$\frac{d\tau}{dt} = M_1 K \left[A_1 \frac{db}{dt} + A_2 \frac{d\Delta}{dt} \right] + M_2 \frac{d\Delta}{dt}$$

Here M_1 and M_2 are an M by N matrices. The boundary conditions are

$$b(t) = b_0 + t \sum_{k=1}^K v_k c_k = b_0 + t C v$$

where the vectors c_k are composed of the indexes of all those boundary displacements that move at velocity v_k . In this case there are only K independent boundary conditions. The time rate of change of stress on the fault elements can be written

$$\frac{d\tau}{dt} = \left[M_1 K^{-1} A_1 C \right] v + \left[M_1 K^{-1} A_2 + M_2 \right] \frac{d\Delta}{dt} \quad (5)$$

These equations with equation 4 completely determine the time evolution of the fault system by $2M$ ordinary differential equations in the shear stress and temperature on the fault elements.

These equations depend on two rather complicated matrix expressions that are actually easy to evaluate. Let $X = K^{-1} A_1 C$ and $Y = K^{-1} A_2$. These matrices have columns which are the solutions of an associated elastic finite element problem for $KX = A_1 C$ and $KY = A_2$. The matrix multiplications are routine once A_1 and A_2 are determined.

Results

It is natural to begin this calculation with the ambient temperature as the initial temperature, and the equilibrium stress state as the initial stress. The equilibrium stress is calculated for known displacement at the left boundary of the model and the initial slip values Δ_0 are taken as zero. We reduce equations (4) and (5) to their nondimensional forms to simplify calculations. There are two assumptions involved in the normalization process. In order to obtain the finite displacement for the infinitely thin

fault, the elastic constant of the interface element is defined so that $Y_1 = \lim_{a \rightarrow 0} \frac{Y}{a}$ remains finite. Y is the

elastic constant of the fault material, and Y_1 is the elastic constant of the one dimensional interface element. Y_1 is so determined that displacement across the interface element (fault) is of the same order of magnitude as the displacement across a normal finite element. Since the stress in an interface element and in a neighboring finite element are of the same order of magnitude, $Y_1 L = Y_c$, where Y_c is the elastic constant of the normal finite elements, and L is the typical length of the interface elements. The length scale L provides the indication of the various processes that may occur in the system and from this argument the average length of the fault elements is the correct scale length. For the elastic moduli assumed here $L = 35 \text{ km}$ is a coarse grain characteristic size of the fault geometry.

The quantities t , τ , Δ and T are reduced to their nondimensional forms by $1/B$, LM_2 , L and $M_2 L^2 / \sigma c_p$, where M_2 is the maximum element of the matrix M_2 . After this normalization

$$\frac{dT}{dt} = \tau \frac{d\Delta}{dt} - (T - T_0)$$

$$\frac{d\Delta}{dt} = \tilde{C} e^{\frac{Q}{T}} \sinh \frac{A\tau}{T}$$

$$\frac{d\tau}{dt} = \tilde{M}_1 v + \tilde{M}_2 \frac{d\Delta}{dt}$$

where t , σ , Δ and T are nondimensional variables, \tilde{C} is $\frac{C}{BL}$, Q is $\frac{E\sigma c_p}{RM_2 L^2}$, A is $\frac{v\sigma c_p}{RL}$, \tilde{M}_1 is

$$\left[M_1 K^{-1} A_1 C \right] / M_2, \text{ and } \tilde{M}_2 \text{ is } \left[M_1 K^{-1} A_2 + M_2 \right] / M_2.$$

\tilde{C} , Q and A can be estimated from the typical physical constants in subducting slabs (Ogawa 1987). In order to determine the surface density σ and one dimensional conductivity K_1 , we need to know $2a$, the thickness of the fault. The thin element approximation requires that the thickness of the fault is much smaller than its length and we chose $a = 0.5\text{km}$. This puts a quite different length scale into the problem. The density ρ is about 3000 kg/m^3 , c_p about 800 J/kg deg , the thermal conductivity K is about 2 to 3 J/m-s-deg , the elastic constant Y is about 70 to 130 GPa , the activation energy E is about 390 to 570 kJ/mole . For the kind of plastic creep normally considered in metallurgy the activation volume is in the range 10^{-7} to $10^{-13}\text{ m}^3/\text{mole}$, since it must be controlled by a length scale of the order of the atomic spacing, 10^{-10}m . In our problem we deal with processes on a much larger scale and estimate the activation volume as the square of the Burger vector of the dislocation times the jog spacing of dislocations. This gives activation volumes on the order of $4 \times 10^{-3}\text{ m}^3$. The atomic vibration frequency $1/c_0$ is of order 10^{12} to 10^{14} . In our one dimensional model, we choose the surface density σ by $\sigma = 2ap$. B varies from $1.3 \times 10^{-11}\text{ s}^{-1}$ to $4.0 \times 10^{-11}\text{ s}^{-1}$, Q varies from 4.6×10^{-2} to 6.7×10^{-2} , A varies from 4.8×10^{-3} to 4.8×10^{-9} . \tilde{C} is of the order of 3.6×10^{20} to 1.1×10^{23} . Most of these numbers are very uncertain and constrained only by observational data that suggest the low stress viscosity of rock is in the range 10^{21} to 10^{28} , so changes to make the system produce realistic earthquake sequences are entirely justified.

The two dimensional finite element model used in this calculation is representative of structure on a line crossing Vancouver Island and perpendicular to the coast of North America (Figure 1). Because the Juan de Fuca plate has moved in a direction $N35^\circ\text{E}$ relative to the America plate for the last million years (Riddihough 1984; Keen and Hyndman 1979), we assumed the driving force on the Juan de Fuca plate would be in this direction. The geometric configuration of our model is mainly based on the results of analysis of LITHOPROBE seismic profiles (Yorath et al. 1985; Green et al. 1986a, 1986b) and the gravity model of that area (Riddihough 1979). Since in a two dimensional elastic model, a bent fault must be accommodated by a more complex structure, we ignored the known sudden increase of the slope of the subducting oceanic plate beneath the continental plate under Vancouver Island and modelled the boundary between the subducting plate and continental plate and upper mantle which we considered a fault zone, by a straight fault of 18° dip.

Figure 2 shows the mesh of the model. The material parameters are those used previously (Nyland and Li 1986). The oceanic plate and the upper mantle beneath it move at a constant velocity along the fault. Such movement corresponds to the push from the Juan de Fuca Ridge or drag from mantle convection. The gravitational pull is not dominant in that area (Nyland and Li 1986). This model was used to calculate the interaction matrix and the time evolution of the dynamics was explored by the modified algorithm discussed above for a variety of fault parameters and initial conditions.

We chose the middle of the plausible range of parameters and integrated the resulting equations using a 12th order Adam's method as implemented in the routine DIVPAG (IMSL, p640 1987). No extraordinary efforts, other than a liberal application of computer time, were required to get solutions over a time interval of 5000 years. The system very quickly settled down to continuous small stress drops on the first and the fourth elements and constant stress constant strain rate creep elsewhere. The shallow seismicity in this case is not a very good simulation of the observed shallow seismicity under the west coast of Canada, but we ascribe this to the coarseness of our model there. It corresponds to depths from

0 to 40km.

The simulation is most sensitive to the choice of activation volume and quite sensitive to the choice of ambient temperature. Small changes here can eliminate the oscillatory pairing we observed on elements one and four and produce a sequence with only shallow seismicity on element one. In spite of extensive attempts we never got activity on the deeper elements with the material parameters discussed above.

It is possible to activate deep elements if we change the initial conditions. It can be argued convincingly that fault zones must have a blocky structure. If this is so the stresses that act at the limited areas of contact between these blocks must be much larger than those that drive the zone as a whole and such stresses are much more likely to be in the plastic regime for the material. When we amplify the initial stresses, by a factor of 10 to stresses on the order of 10^3 bars the numerical integrator encounters points at which the solution is changing so rapidly that it fails. The equation is clearly changing character, becoming stiff. This invariably occurs as temperature is high and rising on one or more fault elements and the stress is high on such elements. We interpret this condition as an indication that failure is imminent on this element and that the equations discussed in the previous section will not be adequate to describe this failure. In this situation we raised the temperature of the interface element until it was possible to calculate the stress drop required to stabilise the time rate of change of stress to zero on this element and continued the integration using this state as a new initial condition.

This is an assumption about the nature of fracturing that occurs in the system. It says that at some point an element melts and that it drops very rapidly to an equilibrium point at the stress level where the time rate of change of stress is zero. Such a ground state must exist, for at instability the time rate of change is negative and during quasistatic loading it is generally positive. Clearly other hypotheses about fracturing could be introduced, but this one is both reasonable and computationally easy to use. Observe that the "instantaneous" nature of the transition means that heat flow cannot play a role and that the energy that appears as a consequence of the stress drop can radiate away as seismic waves. This assumption of 100% seismic efficiency is obviously also open to question.

Conclusions

The assumption that laboratory derived constitutive equations are legitimate for material in fault zones is by no means proved but it is worth testing with simulations. The idea is particularly interesting in an area such as the west coast of Canada and the northwest US. There some speculation suggests an occasional very large thrust earthquake may have occurred. Nevertheless our objective was not to simulate this zone, it was to explore whether temperature dependent non-linear creep laws can generate chaotic seismic sequences. They can, but only with choices of material parameters perceived to be unreasonable in the light of laboratory results. Our preliminary results suggest that shear melting instabilities cannot provide an explanation for deep earthquakes associated with the subduction of the Juan de Fuca plate. This is useful for such earthquakes have not occurred in the short time the area has been monitored and suggests that the holocene geologic evidence for major thrust events on the Cascadia subduction zone (reference) may have another explanation.

It is of course possible that our simulation is inadequate. We have for instance not included the modified behavior of the constitutive equation near melting suggested by Mahboobi

(1981). She points out that the effective viscosity of a fault element is $\eta_{\text{eff}} = \frac{\tau}{\frac{\partial \Delta}{\partial t}} = \frac{\tau c_0 kT}{ac_0 \sinh \frac{v\tau}{kT}}$

and $(\eta_{\text{eff}})_{\tau \rightarrow 0} = \frac{kT}{ac_0 v} e^{\frac{E}{kT}}$ could be identified with any Newtonian process such as the Nabarro-Herring viscosity. As a consequence in microscopic theories of creep, c_0 is related to the range of atomic order in a system and $(\eta_{\text{eff}})_{\tau \rightarrow 0}$ can be constrained to have a limiting low stress viscosity in the form (Tozer 1972) $v_0 P T e^{\frac{A T_m}{T}}$ where $v_0 = B \left\{ \frac{1}{2} L_1 (1 + \tanh c'(T - T_m)) + L_2 \right\}^2$ B is the atomic vibration frequency L_1 can be thought of as the grain size of material at sub solidus temperatures and L_2 as the interatomic distance in the liquid phase and c' is an adjustable parameter determining the melting range.

To take account of the effects of grinding and annealing which may occur in the process of faulting L_1 , the grain size of material at subsolidus temperatures, is not treated as a constant. Normal stress, strain and temperature are factors involved in controlling the grain size of the material in a faulting process (Engedler 1974, Anderson et al. 1980, Phillips 1982, Anderson et al. 1983, Sammis et al. 1986). The rate of change of L_1 can be formalized as

$$\frac{dL_1}{dt} = \alpha [L_1 - L_{\min}] \frac{\partial \Delta}{\partial t} - \frac{(L_1 - L_{\max})}{\tau_0}$$

normal stresses and L_{\min} is the minimum grain size obtained as a result of grinding. Its lowest value has been estimated to be of the order of 10^{-9} m (Lowrison 1974). The second term in the right hand side of the above equation is the annealing term. L_{\max} is the limiting size that the material tend to grow as a result of annealing and τ_0 is a relaxation time defined as $\tau_0 = 10^6 \frac{A T_m}{e T}$.

The difficulty with this argument is that for conditions in a subduction zone the values of the parameters are most uncertain and almost any result could be generated with it. There are really only two ways to constrain this kind of modelling other than the desire to make the material parameters "reasonable". The resulting seismicity catalog should be an adequate representation of the actually observed behaviour and the deformation in the system should be similar to that actually observed in the area. We have a model that predicts the essentially shallow seismicity in the area and can run this model for 5000 years without seeing a major thrust earthquake. With the limited resolution of the model we cannot predict details of the shallow seismicity catalog. In any case such details are likely to be the consequence of more processes than thermally controlled non-linear creep. We have not done the calculations required to predict surface strain and to compare it with the known compression parallel the subduction direction and tilting of the overthrust plate towards the underthrust one. Such macro constraints may fix the activation volume, and possibly correct the initial stress states for the simulation.

Acknowledgements

This work was begun while AMG visited University of Alberta from the Institute for Physics of the Earth in Moscow, USSR. The rheology of the fault zones and methods of computing their evolution were derived from the doctoral thesis done by NN at University of Newcastle on Tyne after an undergraduate education in Iran. QL is a graduate student at Alberta from the People's Republic of China. EN is grateful to uncounted bureaucracies for the opportunity to put together this group. We are also grateful to the Natural Sciences and Engineering Research Council of Canada and the Alberta Oil Sands Technology and Research Authority for support

References

- Cook, R. D. 1981. Concepts and Applications of Finite Element Analysis. by John Wiley & Sons, Inc.
- Gabrielov A.M., V.I. Keilis-Borok, T.A. Levshina, V.A. Shaposhnikov, Block model of dynamics of the lithosphere, Computational Seismology, 19, pp 168-177, Moscow Nauka, in Russian
- Green, A. G., Berry, M. J., Spencer, C. P., Kanasevich, E. R., Chiu, S., Clowes, R. M., Yorath, C. J., Stewart, D. B., Unger, J. D., and Poole, W. H. 1986b. Recent seismic reflection studies in Canada. American Geophysical Union, Geodynamics Series, Vol 13, pp. 85-97.
- Green, A. G., Clowes, R. M., Yorath, C. J., Spencer, C., Kanasevich, E. R., Brandon, M. T., and Brown, A. S. 1986a. Reflection mapping underplated oceanic lithosphere and the subducting Juan de Fuca plate. Nature (London), 319, pp.210-213.
- IMSL, Math/Library user's manual version 1.0, IMSL Inc., April 1987
- Keen, C. E., and Hyndman, R. D. 1979. Geophysical review of the continental margins of eastern and western Canada. Canadian Journal of Earth Sciences, 16, pp. 712-747.
- Keilis-Borok V.I., and V.G. Kosobokov, Time of Increased Probability for the Great Earthquakes of the World, Computational Seismology, 19, pp 48-57, Moscow, Nauka, in Russian
- Li, Q. 1986. Analysis of Seismic Instability of the Vancouver Island Lithoprobe Transect. M.Sc. Thesis, The University of Alberta, Edmonton.
- Nyland, E., and Li, Q. 1986. Analysis of seismic instability of the Vancouver Island lithoprobe transect. Canadian Journal of Earth Sciences, 23, pp.2057-2067.
- Ogawa M., 1987 Shear Instability in a Viscoelastic Material as the Cause of Deep Focus Earthquakes, Journal of Geophysical Research, 92, B13, pp13801-13810
- Riddihough, R. P. 1979. Gravity and structure of an active margin-British Columbia and Washington. Canadian Journal of Earth Sciences, 14, pp. 384-396.
- Riddihough, R. P. 1984. Recent movements of the Juan de Fuca plate system. Journal of Geophysical Research, 89, pp. 6980-6994.
- Sadovsky M.A., L.G. Bolhovitinov L.G., V.F. Pisarenko, On the property of discreteness of the rocks, Proc. Ac. Sci. USSR, Physics of the Earth, 1982, no 12, pp3-19, (in Russian)
- Yorath, R. M., Clowes, R. M., Brown, A. S., Brandon, M. T., Massey, N. W. D., Green, A. G., Spencer, C., Kanasevich, E. R., and Hyndman, R. D. 1985. Lithoprobe phase 1: southern Vancouver Island: preliminary analyses of reflection seismic profiles and surface geological studies. In Current research, part A. Geological Survey of Canada, Paper 85-1A, pp. 543-554.4.

A Linear Creep Model of Aftershocks

Qing Li, Yuchun Wang and Edo Nyland

Department of Physics
University of Alberta
Edmonton, Alberta, Canada
T6G 2J1

Preliminary and Subject to Revision

Abstract

A study of the detailed earthquake catalog of North Central China shows that the curve of cumulative energy released during the aftershock sequences of Haicheng earthquake, February 4, 1975 and Tangshan earthquake, July 28, 1976 are characterized by several straight line segments when the time axis is logarithmic. A linear viscoelastic model can therefore explain portions of the aftershock sequence as a time relaxation process. Here we apply the logarithmic creep law to a large volume of shear strained and fractured material. The frequency independent Q implied in seismic frequency range by these data is 450 for Haicheng area and 200 for Tangshan area.

1. Introduction

Seismic behavior in an area is directly related to the local geological environment and material properties. Numerical models of subduction in the Middle America Trench and beneath Vancouver Island have exploited the relationships between stress concentrations and geological structures (Uribe 1984; Nyland and Li 1987). The barrier and asperity model relates the characteristics of earthquake patterns to the mechanical properties of the region (Kanamori 1981). All this suggests that the features of earthquake sequences are sensitive to mechanical properties of local lithospheric material. Generally it is not sufficient to consider the earth elastic when we deal with earthquake processes. Surface displacement and their temporal development immediately after an earthquake have been observed by geodetic measurements. An elastic rebound theory to explain this effect was first proposed by H. F. Reid in 1911. Recently more studies have been done on such subject (Lang et al., 1984; Melosh and Raefsky, 1983).

Earthquake sequences occur in different patterns which vary from region to region. These patterns, such as seismic gaps, bursts of seismicity and migration, have been intensively studied by a number of seismologists, and may be precursors of strong earthquakes (Mogi 1979; Keilis-Borok et al. 1980 a, b, c; Lamoreaux 1982). Their physical causes are not fully understood, but some statistical and mechanical models of earthquakes may give qualitative explanations for these patterns (Kagan and Knopoff 1976; Aki 1979; Kanamori 1981; Barenblatt, Keilis-Borok and Vishik 1981).

The most evident feature of an earthquake catalog consists of aftershocks produced by strong earthquakes. The behavior of aftershocks are as complicated and varied from region to region as those of mainshocks but their three major characteristics are: (a) the number of aftershocks per day decreases with time, which is formulated as Omori's law; (b) the energy released per day decreases with time; (c) the duration of aftershock sequences depends on the magnitude of mainshocks and is very short compared with recurrence time of mainshocks. These properties show that aftershocks are local effects in time, they may be excluded from analysis of the overall dynamics of the lithosphere. However, we need a better understanding of aftershocks before we remove them from the catalog.

Recent development in the field of deterministic chaos may provide a convenient tool for this analysis for it allows us to consider the dynamics of lithosphere as a deterministic system. By coarse graining the lithosphere, its dynamics can in principle be described in a high dimensional phase space and an earthquake catalog corresponds to a collection of the points on a specially chosen Poincare section (reference???) of this space. The return times of the lithospheric phase space trajectory crossing this Poincare section correspond to the time intervals between successive seismic events (Li and Nyland 1988). Thermal instability models have shown that the erratic behavior of the earthquake catalog could be caused by nonlinear coupling among a group of processes which describe the dynamics of the system. Such coupling effects correspond to the interactions between different fault segments (Gabrielov et al. 1988).

To fully understand aftershock sequences we need knowledge of geological structure and the properties of the materials where aftershocks occur, and the knowledge of physical laws which governs fracture processes. It seems, therefore, the study of aftershock sequences is not easier than the study of mainshock sequences, which is now far from being understood. As long as we do not demand detailed knowledge of the earthquake generating process but are content with estimates of the rate of energy release it is possible to extract information from a model of a fractured region that is described in an average, rather than an exact way. The processes we consider, the main shock and its associated aftershocks, occur in a volume of the lithosphere which could degenerate to a fault plane but is not required to do so. The aftershock sequence is caused by fluctuations of stress about its mean value in this volume. It is the mechanical properties of this volume which

affect the aftershock sequence.

One of advantages in analysing aftershock sequences is that their driven mechanism can be estimated. We approach this problem by examine the energy released during the aftershock sequences. This approach certainly will involve some assumptions and we can only obtain a part of knowledge of the aftershock process. Our purpose is to get some fundamental insight into how the rheology of the materials influence the aftershock sequences from this model which we try to make it simple. This is general philosophy in modelling problem.

We have investigated the features of two aftershock sequences. The main shocks occurred on February 4, 1975, with magnitude 7.3 at Haicheng, and July 28, 1976, with magnitude 7.8 at Tangshan, People's Republic of China. We explain the energy released during these aftershock sequences with a linear creep model. In order to study these processes we use an earthquake catalog containing the events identified by China's national seismic network from 1970 to 1984 in North Central China. Since 1966, seismic monitoring has been greatly enhanced in our study area and the aftershock sequences of the Haicheng and Tangshan earthquakes are well documented, probably to a magnitude threshold of 1 on Richter Scale. Certainly, not all small magnitude earthquakes are present in the catalog.

In solid materials the properties of transient creep, internal friction and dispersion, can be correlated on the basis of a linear theory, which certainly applies for the small strain case. Creep tests in igneous rocks indicates the existence of such a linear region for rocks (Lomnitz 1956, 1957). The logarithmic creep function for rocks was also proposed by Lomnitz. In this paper we assume a linear model with a logarithmic creep law applied to a volume a few kilometers in linear dimension can explain the energy released during the aftershock sequences.

The imperfection of this medium is well known to cause seismic wave amplitude attenuation, described by quality factor Q . These effects mainly relate to anelasticity and inhomogeneity of the material, the first converts elastic energy to heat and the second scatters the energy away from the direction of propagation. The factor Q calculated for Haicheng and Tangshan area with our model only relates to the first effect. These values therefore may be higher than those determined from analysis of seismic waves which include scattering effects due to randomly distributed scatterers (Aki, 1969, 1975).

2. Creep and Aftershocks

The studies of creep and seismicity supported models suggesting that creep occurs in such a manner as to load relatively strong areas or asperities within the fault zone that subsequently fail in earthquakes (Wesson 1988). Laboratory studies of creep deformation of rocks and other solid materials under conditions appropriate to brittle fracture show a remarkable uniformity of behavior. Three stages of creep deformation are displayed as the materials stressed close to the breaking point. The primary creep is a transient stage of response associated with the application of the load. Secondary creep is a steady respond, the slope is approximately constant. The tertiary phase is an accelerating process that culminates in the catastrophe of fracture. Some phases disappear when the shear stress and the temperature vary in the experiments. The empirical creep laws have been suggested for first and second stages, the tertiary stage is less understood.

The most commonly used empirical creep law are power law and logarithmic law. They provide useful representations of experimental data in transient and steady-state creep. When the stress and temperature are rather low, the materials generally obey the logarithmic law. These conditions are not unlike those under which shallow earthquakes occur. Underground experiments shows good agreement with logarithmic creep. In flat-jack measurement, the creep between pins of flat-jack after cutting the slot into a rock behaves logarithmically.

Such situation is close to the relaxation of a region after a strong earthquake which released a certain amount of stress.

The logarithmic creep law

$$\Phi(t) = a \ln(1 + \alpha t)$$

where a and α are two constants depends on the conditions of experiments. The constant α , which has dimension of frequency, appears to be related to the frequency of vibration of a vacancy in the crystal lattice. It has a value of 10^3 Hz for a creep test of igneous rocks, and ranges from 10^{10} to 10^{14} Hz from theoretical consideration of metals.

Power law creep function is also suggested for rocks. The commonly used form is given by Jeffreys (1958)

$$\Phi(t) = a \left[(1 + \alpha t)^\beta - 1 \right]$$

where a , α and β are three constants. Some other creep laws have been derived from simple linear rheologic models visualized as linear combinations of springs and dashpots. For a standard linear solid, the creep function is

$$\Phi(t) = \left(\frac{\tau_\sigma}{\tau_\epsilon} - 1 \right) \left(1 - e^{-\frac{t}{\tau_\sigma}} \right)$$

where τ_ϵ and τ_σ are characteristic relaxation time of strain and stress respectively.

Earthquake occurrence can be treated as a stress accumulation and release process. Due to tectonic movement in an area, shear stress and strain increase with time around faults. A strong earthquake happens when the stress exceeds the strength of the fault zone described in term of asperities or equivalent barriers (Kanamori 1981), or the fault system becomes unstable as described by instability model (Rudnicki 1988; Ogawa 1987; Gabrielov et al. 1988). The elastic strain energy stored in the medium around the fault releases immediately and the stress in the area drops from a high level to a low level.

Immediately after the earthquake, the deviatoric stress starts to relax by viscous creep. This stress relaxation leads to the stress redistribution in the fault zone. The stress will concentrated on some unbroken section or the weak zones of the subfaults newly caused by the mainshock or some other area with a local structure anomaly. These places are the candidates for the future fractures. As such a relaxation process goes on, an aftershock will release the strain energy by the failure of those sections. An aftershock sequence generally last two to three years following a strong earthquake. The strain energy released during this period is mainly remaining strain energy of the strong earthquake.

H. F. Reid in 1911 suggested such anelastic relaxation following an elastic break in his elastic rebound theory. Figure 1a illustrates such a process. The line AOB is marked just before a strong earthquake. During this stage, the elastic rebound happens. The AOB break into two parts: AC and BD. The elastic strain energy releases in this stage. During the second stage, the curve AC changes to AC' and BD to BD', the strain energy releases by means of an aftershock sequence governed by anelastic properties of the material. In this paper we focus on the second stage of the strain energy relief. The increase of strain energy due to tectonic motion can be neglected in such a short period. This process are influenced by the lithosphere and asthenosphere rheology

as well as local geological structure (Lang et al., 1984)

We generally identify aftershocks as statistically dependent events following main shocks. They happen in spatial and temporal windows determined by the main shocks. Physically, they might be explained as a stress distribution readjustment and release process after mainshocks. The features of aftershocks vary from region to region due to the inhomogeneity of the media. Their behavior is erratic although statistically the number of aftershocks decreases with time as in Omori's law.

Mathematical modelling has shown that such erratic behavior can be due to nonlinear interaction between different fault segments. In this paper we consider an aftershock sequence as a stress relaxation process due to the anelasticity of the material which indicates that it might depend on the entire history of loading and unloading. The strain energy released during the aftershock sequence consists of the energy stored in the region less the energy released by a mainshock, which is treated as an elastic break in that area. A remarkable fact of this consideration is that the driving force of the dynamic system of aftershocks is governed by the visco-elastic properties of the lithosphere. The energy supplied by the driving force will equal the energy dissipated by the system in term of aftershocks.

Figure 1b illustrates such a process with a simple springs and dashpots model. The relief of strain energy consists of two stages, an elastic break followed by an anelastic relaxation. Before a strong earthquake, the strain energy is stored in the fault zone, i.e. stored in spring k_1 and k_2 . During the elastic break, the elastic strain energy stored in spring k_1 is released. The stress σ drops to a lower level. The relaxation start immediately after the earthquake. In this stage the energy stored in spring k_2 starts to release, and stress σ will increase. When stress σ drops again, a sequence of aftershocks will be generated. The relaxation process is governed by anelastic properties of the material, or the properties of the dashpot.

After a strong earthquake the stress state drops to a low level. If such stress fluctuates around a constant value during the redistribution process, the relation of the cumulative strain energy released in the aftershocks to time can be easily calculated. Although such approximation may not be true, the following study on Tangshan and Haicheng earthquakes suggests that this approximation is applicable to these areas.

3. Catalog Analysis

The catalog used in this paper contains events that occurred in North Central China from 1970 to 1984. The magnitude of the recorded events range upwards from 1.0, and the catalog has detailed records of the aftershock sequences of 1975 Haicheng earthquake and 1976 Tangshan earthquake. Epicenters of large earthquakes in this study are shown in Figure 3 as circles. The big circle at Haicheng shows the event of February 4, 1975 with magnitude of 7.3. The three circles at Tangshan represent events that happened on the same day, July 28, 1976 with magnitudes of 7.8, 7.1 and 6.5 respectively.

An aftershock sequence consists of events physically related to the main event. Unfortunately, the physical causal relationship between the mainshock and its aftershocks has not been fully understood so far. Only some empirical relations have been drawn out. To extract the aftershock sequence of a mainshock from the catalog, we have to define a somewhat arbitrary criteria. Generally we consider two events with time sequence number i and j , $i > j$. The second is an aftershock of the first if and only if the following conditions are satisfied: (1) the distance between their epicenters is less than $R(M_j)$; (2) the time difference $t_i - t_j \leq T(M_j)$; and; (3) $M_i < M_j$. $T(M_j)$ and $R(M_j)$ are empirical functions which can be viewed as simple box car windows containing obvious "mainshock-aftershock" clustering (Lamorex 1982). Gardner and Knopoff (1974) gave a logarithmic relations between time T and magnitude M_j ; and distance R and M_j . Table 1. lists the relationships used as

time and space windows for the identification of aftershock sequences in this study.

Table 1 Windows for identification of aftershocks

M	R(km)	T(days)
6.0	54.0	510.0
6.5	61.0	790.0
7.0	70.0	915.0
7.5	81.0	960.0
8.0	94.0	985.0

Figure 4 shows the cumulative strain energy released in the aftershock sequence of Haicheng earthquake of magnitude of 7.3, February 4, 1975. The abscissa is time plotted logarithmically for the reason which will be discussed in next section. 928 aftershocks were identified with the criteria given in the table 1. The pattern of the Haicheng earthquake is characterized as a single mainshock followed by an aftershock sequence dominated by a number of intermediate earthquakes, about 4.0 to 5.0 in magnitude. The energy was calculated with $\log E = 1.5M + 11.8$

Two straight segments in figure 4, correspond to two periods of seismic activity in the area. The jump at about 200 days after the mainshock corresponds to a 5.4 magnitude event on August 28 of the same year. The similar analysis was done for the aftershock sequence of Tangshan earthquake, magnitude of 7.8, July 28, 1976. Figure 5 shows the cumulative energy released in the aftershock sequence. Following the mainshock two other events of magnitude of 6.5 and 7.1 happened on the same day. These two are responsible for the great jump in the cumulative energy curve on the first day. Two straight segments denoted by AB and CD show clearly in the figure. The jump following the segments corresponds to the event of magnitude 6.5, May 12, 1977.

4. Linear Viscoelastic Models

It is well known fact that earthquakes are associated with a nonlinear process, however, in the relaxation of the earth after an earthquake, a linear viscoelastic model might be applicable. So far we don't have any in situ experimental results showing us what kind of constitutive law we should apply to the lithosphere. We chose a linear viscoelastic model in this study because of its mathematical simplicity, and also because the creep law will become Newtonian when the stress is low (Gabrielov 1988). The stress concentration which initiates an earthquake is a local effect so it is reasonable to consider the stress state of the entire region is low. Numerical modeling shows that linear and nonlinear viscoelastic rheologies do not give substantial different results for the pattern of stress field after an earthquake so the linear viscoelastic model is a good approximation when we deal with relaxation of the earth after an earthquake.

For viscoelastic material there is an instantaneous strain and a time dependent contribution to strain in response to applied stress. When stress $\sigma_{ij}(t)$, a function of time, is applied to a viscoelastic solid initially free of strain and stress, the resulting strain in a linear medium may expressed as a convolution (Aki and Richards 1980; Fung 1965):

$$e_{ij}(t) = E_{ijkl} \sigma_{kl}(t) + \int_{-\infty}^t \sigma_{kl}(\tau) \Phi_{ijkl}(t - \tau) d\tau$$

Where E_{ijkl} is an elastic modulus, and Φ_{ijkl} is known as the creep function. For an isotropic medium, the fourth-order tensor Φ_{ijkl} can be written as

$$\Phi_{ijkl}(t) = \frac{\Phi_2 - \Phi_1}{3} \delta_{ij} \delta_{kl} + \frac{\Phi_1}{2} (\delta_{ik} \delta_{jl} + \delta_{il} \delta_{jk})$$

Where Φ_1 and Φ_2 are scalar functions. Φ_1 is the shear strain creep function and Φ_2 the dilatational strain creep function. Therefore the strain and stress relation can be described as

$$e_{ij}(t) = E_{ijkl} \sigma_{kl}(t) + \int_{-\infty}^t \left[\frac{\Phi_2(t-\tau)}{3} \sigma_{kk}(\tau) \delta_{ij} + \Phi_1(t-\tau) \left(\sigma_{ij}(\tau) - \frac{1}{3} \sigma_{kk}(\tau) \delta_{ij} \right) \right] d\tau$$

The first term inside the integration is the confining pressure, and the second term is the deviatoric stress. If an earthquake is a shear failure, we can assume that after the earthquake, the shear stress drops to a lower level, but the confining pressure remains essentially the same. Therefore, the first term inside of integration can be omitted in the following discussion.

We consider a region loaded to a level $\sigma_{ij}^{(1)}$ since time $-T$. At time $t = 0$, the stress suddenly drops to a lower level, which corresponds a mainshock. After the mainshock a number of subfaults are generated, or activated. The strength of the material in that region therefore becomes lower. The remaining strain energy releases successively in aftershocks.

According to the above discussion, the energy released by an aftershock sequence is equal to the energy released during the relaxation following the strong earthquake. It can be written as

$$\Delta E = - \int_V dV \int_0^t \sigma_{ij}(t) de_{ij}(t)$$

We assume that the lower level stress fluctuates around its mean value during the relaxation period, ie. we can express the stress as $\sigma_{ij}(t) = \sigma_{ij}^{(2)} + \delta\sigma_{ij}(t)$. The above integration is then

$$e_{ij}(t) = \int_0^t \left(\sigma_{ij}^{(2)} - \frac{1}{3} \sigma_{kk}^{(2)} \delta_{ij} \right) \dot{\Phi}_1(t-\tau) d\tau + \int_{-\infty}^0 \left(\sigma_{ij}(\tau) - \frac{1}{3} \sigma_{kk}(\tau) \delta_{ij} \right) \dot{\Phi}_1(t-\tau) d\tau$$

$\int_0^t \delta\sigma_{ij}(\tau) f(\tau) d\tau = 0$ if $\delta\sigma_{ij}(t)$ and the function $f(t)$ are not correlated. This applies if f is a creep function and ??? is the stress fluctuation ???.

$$= - \int_V \left(\sigma_{ij}^{(2)} - \frac{1}{3} \sigma_{kk}^{(2)} \delta_{ij} \right) \left[\int_{-\infty}^t \left(\sigma_{ij}(\tau) - \frac{1}{3} \sigma_{kk}(\tau) \delta_{ij} \right) \dot{\Phi}_1(t-\tau) d\tau - \int_{-\infty}^0 \left(\sigma_{ij}(\tau) - \frac{1}{3} \sigma_{kk}(\tau) \delta_{ij} \right) \dot{\Phi}_1(t-\tau) d\tau \right] dV$$

$$= - \int_V \left(\sigma_{ij}^{(2)} - \frac{1}{3} \sigma_{ii}^{(2)} \delta_{ij} \right) \left[\int_0^t \left(\sigma_{ij}(\tau) - \frac{1}{3} \sigma_{ii}(\tau) \delta_{ij} \right) \dot{\Phi}_1(t-\tau) d\tau + \int_{-T}^0 \left(\sigma_{ij}(\tau) - \frac{1}{3} \sigma_{ii}(\tau) \delta_{ij} \right) \left(\dot{\Phi}_1(t-\tau) - \dot{\Phi}_1(-\tau) \right) d\tau \right] dv$$

Since the recurrence time interval is much larger than aftershock duration, ie. the loading process is much longer than the transient period of creep, we can take the approximation $\dot{\Phi}_1(t-\tau) - \dot{\Phi}_1(-\tau) = 0$ when $t < -T$. We then have

$$\Delta E = \int_V \left[\sigma^{(2)} \sigma^{(1)} (\Phi(T) - \Phi(T-t)) + \sigma^{(2)} \Delta \sigma \Phi(t) \right] dv$$

where $\Delta \sigma = \sigma^{(1)} - \sigma^{(2)}$. For the reason of simplicity, the deviatoric stress is denoted by σ in above expression, and will be so for rest of this paper. Again with the approximation

$\Phi(T+t) - \Phi(T) = 0$, we have

$$\Delta E = V \sigma^{(2)} \Delta \sigma \Phi(t)$$

where V is the volume within which the stress drop due to the mainshock is significant. The over bar indicates volume average. This relation shows the energy released in aftershocks is directly related to the creep function of the lithosphere. Therefore the cumulative energy released in aftershocks as a function of time indicates what kind of creep function we should use to describe the lithosphere.

The linear relationship between energy E and logarithmic time T shown in Figure 4 and 5 suggest logarithmic creep, which was deduced from laboratory measurements on intact specimens and gives better agreement with experimental data than other models. We have tried the power law creep function and the creep function for the standard solid to match the energy released in aftershocks, it shows larger deviation. The increase of the slope of the straight segment CD (Figure 4) can be explained by the superposition of the energy due to the aftershock of the mainshock and that due to the event at August 28, 1975, with magnitude of 5.8. This quake may have been triggered by the mainshock, but the stress level of that region may have not dropped to $\sigma^{(2)}$ after the mainshock. In other words, the strain energy released in this event is not due to the anelastic part of energy stored in the region. Although this event may have a causal relationship to the main event, the mechanism must be different from other aftershocks. The same explanation can be applied to Figure 5.

We have to emphasize that most experiments, such as flat jack underground experiments, on which the logarithmic creep law is based are carried out to measure dilatational strain creep phenomena. For an earthquake process, shear strain relief is dominant. In the analysis of this paper, only the shear strain creep function is concerned in our energy budget. The results of this paper are thus obviously restricted to the case of material which suffers shear stress.

5. Estimates of Q

Due to the "internal friction" of material, seismic wave amplitudes will attenuate when a seismic disturbance propagates through the media. Such materials are said to be anelastic and generally described by viscoelasticity. The measure of the internal friction is the dimensionless quantity Q , which is defined by the

ratio of the peak strain energy stored in the specimen and the energy dissipated in each cycle.

$$\frac{1}{Q} = \frac{\Delta E}{2\pi E}$$

The seismic quality factor Q is strictly frequency dependent because of causality, but it is observed to be effectively constant over the wide range of frequencies observed in seismology (0.001 -- 100 Hz). The logarithmic creep law implies an effectively frequency independent Q under the condition $\omega \ll \alpha$, and $q \ll 1$ (Aki and Richards 1980)

$$\frac{1}{Q} \approx \frac{\pi q}{2}$$

Here q is one of two parameters of creep function is equal to $2\mu a$ in our expression. Their result is applicable to our discussion.

We have an expression for the energy released during aftershock sequences in terms of logarithmic creep law:

$$\Delta E = A \ln(1 + \alpha t)$$

where $A = \frac{1}{2} V \sigma^{(2)} \Delta \sigma$, $\sigma^{(2)}$ is final state of pure shear stress after the mainshock, $\Delta \sigma$ is the pure shear stress drop during the mainshock. The energy released in the mainshock is

$$E_{\text{main}} = \frac{1}{2} V (\sigma^{(1)} + \sigma^{(2)}) \frac{\Delta \sigma}{2\mu}$$

Therefore, we can express q by

$$q = \left(1 + \frac{\sigma^{(1)}}{\sigma^{(2)}} \right) \frac{A}{E_{\text{main}}}$$

To calculate q , we need to know stress states before and after the earthquake.

??? We therefore are justified in taking the zero-th approximation for q

$$q = \frac{2A}{E_{\text{main}}}$$

With known q , Q can be easily calculated.

$$\frac{1}{Q} \approx \frac{\pi A}{E_{\text{main}}}$$

Since we have approximate expression for ΔE :

$$\Delta E \approx A \ln \alpha + A \ln t$$

(the approximation is valid when $\alpha t \gg 1$), two parameters A and α can be determined by the slopes of the segments and their intercepts with the energy axis. The slope of segment AB in Figure 4 is 0.4×10^{20} ergs/ln(day) and the intercept is 11.76×10^{20} ergs. The parameters q and a are calculated to be 0.0014 and 6.8×10^7 Hz, which satisfy the approximation conditions used to derive the effectively frequency independent Q .

The factor Q calculated for Haicheng area is 450.

The same analysis is carried out for Tangshan region. Since the events of magnitude 6.5 and 7.1 happened on the same day as the mainshock, we take the energy released by these three events as the value for E_{main} in the formula. The q and Q are calculated to be 0.003 and 200 respectively.

Li and Gu (1980) have calculated Q by means of the amplitude of \bar{P} arrivals recorded at many stations in the Haicheng area. The average Q they find is 530 for upper crust of Haicheng region. The Q_L for lithosphere is calculated from the aftershock data of Tangshan earthquake, which is recorded by the stations at Haicheng area. The Q_L value of 200, gives the average effect of the lithosphere under Tangshan and Haicheng area. The mainshocks of Haicheng and Tangshan have the depth of 12 and 16 km, respectively. The Q we obtained for Haicheng area may be influenced by the effect of upper crust which has a high Q .

If we include the effect of the efficiency of seismic wave radiation, the Q will be modified by the factor $\frac{\eta_{\text{after}}}{\eta_{\text{main}}}$,

where η_{after} and η_{main} represent seismic efficiencies for aftershock and mainshock respectively. The Q will decrease if η_{after} is smaller than η_{main} .

Again we have to emphasize that since the creep function participated in the analysis is the shear strain creep function, the dimensionless quantity Q determined above is only valid for shear wave propagation through the media.

6. Conclusion

From the analysis of two recent earthquakes in North Central China, we can successfully explain the aftershock sequences as relaxation processes. The features of such processes depend on the anelastic properties of local lithosphere. The curves of cumulative energy released during the aftershock sequences are characterized by several straight segments. These results imply that besides the simple definition of aftershock events from space and time causal relations, we can classify the aftershock events as two kinds: one is due to the relief of strain energy which stored in the medium and can not be released suddenly with an elastic break; the other is due to the break of some unbroken sections where the stress level did not drop to a lower level after the mainshock. This classification will help us to distinguish the aftershock events of two different mechanisms.

The analysis supports the notion that the energy released during aftershock sequences can be explained by a linear creep model. This suggests that the logarithmic creep law can be applied to large scale shear strained and fractured body as well as to laboratory scale samples. The two parameters in the creep function estimated from our model of aftershock sequences are in reasonable agreement with the experimental results. The dimensionless quantity Q estimated with this model has a value of 450 for Haicheng area and 200 for Tangshan area. These estimates are high, but they include only the dissipative, not the scattering part of Q .

Acknowledgements

The work in this paper is part of a study of the geomechanical implications of microseismicity supported jointly by the Natural Sciences and Engineering Research Council of Canada and the Alberta Oil Sands Research Authority.

References

- Aki, K., and P. G. Richards, *Quantitative Seismology Theory and Methods*, W. H. Freeman and Company, Vol 1, 177-181, 1980
- Aki, K., Analysis of the seismic coda of local earthquake as scattered waves, *J. Geophys. Res.*, Vol 74, 615-631, 1969
- Aki, K., and B. Chouet, Origin of coda waves: Source, attenuation, and scattering effects, *J. Geophys. Res.*, Vol 80, 3332-3342, 1975
- Barenblatt, G. I., V. I. Keilis-Borok, and M. M. Vishik, A model of the clustering of earthquakes, *Proc. Natl. Acad. Sci. USA*, Vol 78, 5284 - 5287, 1981
- Brace, W. F., D. L. Kohlstedt, Limits on lithospheric stress imposed by laboratory experiments, *J. Geophys. Res.*, Vol. 85, 6248-6252, 1980
- Feng, Y. C., *Foundations of solid mechanics*, Prentice-Hall Inc., 1965
- Gardner, J. S., and L. Knopoff, Is the sequence of earthquakes in southern California, with aftershocks removed Poissonian?, *Bull. Seismol. Soc. Amer.*, Vol 64, 1363-1367, 1974
- Li, X. C., and H. D. Gu, On the attenuation of seismic waves through the Haicheng earthquake area, *Acta Seismologica Sinica*, Vol. 2, No. 4, 1980 (in Chinese)
- Jeffreys, H., A modification of Lomnitz's law of creep in rocks, *Geophys. J.*, Vol 1, 92-95, 1958
- Kagan, Y., and L. Knopoff, Statistical search for non-random features of seismicity of strong earthquakes, *Phys. Earth Planet Interiors*, Vol 12, 291 - 318, 1976
- Kanamori, H., The nature of seismicity patterns before large earthquakes, *Maurice Ewing Series*, Vol. 4, AGU, 1981
- Kanamori, H., and D. L. Anderson, Theoretical basis of some empirical relations in seismology, *Bull. Seismol. Soc. Amer.*, Vol. 65, 1073-1095, 1975
- Keilis-Borok, V. I., L. Knopoff, and I. M. Rotvain, Bursts of aftershocks, long-term precursors of strong earthquakes, *Nature*, Vol 283, 259 - 263, 1980a
- Keilis-Borok, V. I., L. Knopoff, I. M. Rotvain and T. M. Sidorenko, Bursts of seismicity as long-term precursors of strong earthquakes, *J. Geophys. Res.* Vol 85, 803 - 811, 1980b
- Keilis-Borok, V. I., L. Knopoff, and C. R. Allen, long-term premonitory seismicity patterns in Tibet and the Himalayas, *J. Geophys. Res.* Vol 85, 813 - 820, 1980c
- Lamoreaux, R. D., *Cluster Patterns in Seismicity*, Ph.D. thesis, University of Alberta, Edmonton, 1982
- Lomnitz, C., Creep measurements in igneous rocks, *J. Geol.*, Vol. 64, 473, 1956
- Lomnitz, C., Linear dissipation in solid, *J. Appl. Phys.*, Vol 28, 201-205, 1957
- Mogi, K., Two kinds of gaps, *Pure and Appl. Geophys.*, Vol 117, 1172 - 1186, 1979
- Nyland, E., and Q. Li, Analysis of seismic instability of the Vancouver Island lithoprobe transect, *Can. J. Earth Sci.*, Vol 23, 2057-2067, 1987
- Shmazaki, K., and T. Nakata, Time-predictable recurrence model for large earthquakes, *Geophys. Res. Lett.*, Vol 7, 279-282, 1980
- Uribe-Carvajal, A., *Seismic stability studies near the middle america trench*, Ph.D. thesis, University of Alberta, Edmonton, 1984

List of Figures

Figure 1 --- a simple model to illustrate recurrence of earthquakes. (a) shows stress accumulation and drop. (b) shows cumulative energy release during each earthquakes.

Figure 2 --- an elastic rebound and relaxation model. Different curves correspond to different stages of earthquake process.

Figure 3 --- a map of epicenter location of Haicheng earthquake, February 4, 1975; and Tangshan earthquake, July 28, 1976.

Figure 4 --- cumulative energy released in the aftershocks of Haicheng earthquake in February 4, 1975

Figure 5 --- cumulative energy released in the aftershocks of Tangshan earthquake in July 28, 1976

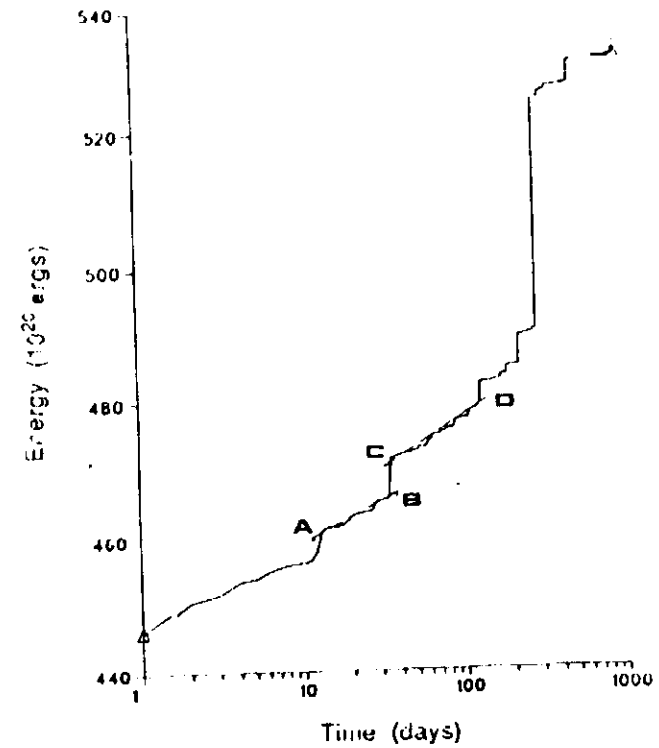


Figure 5

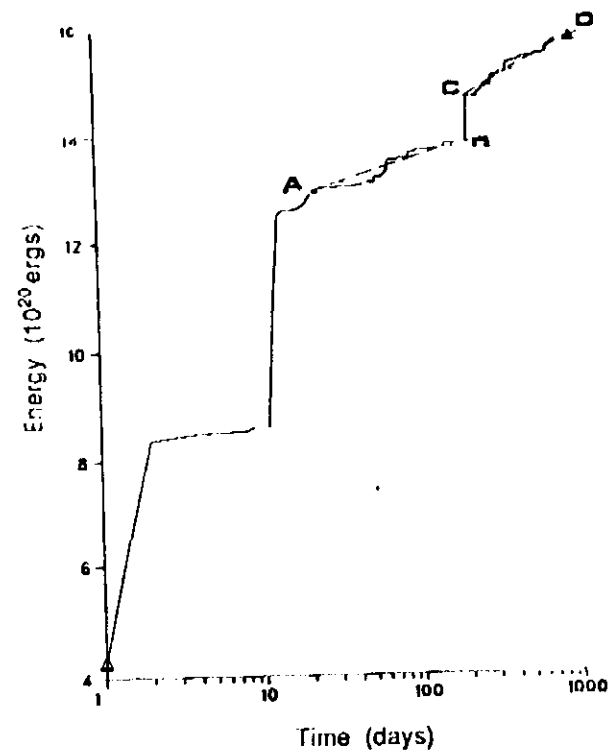
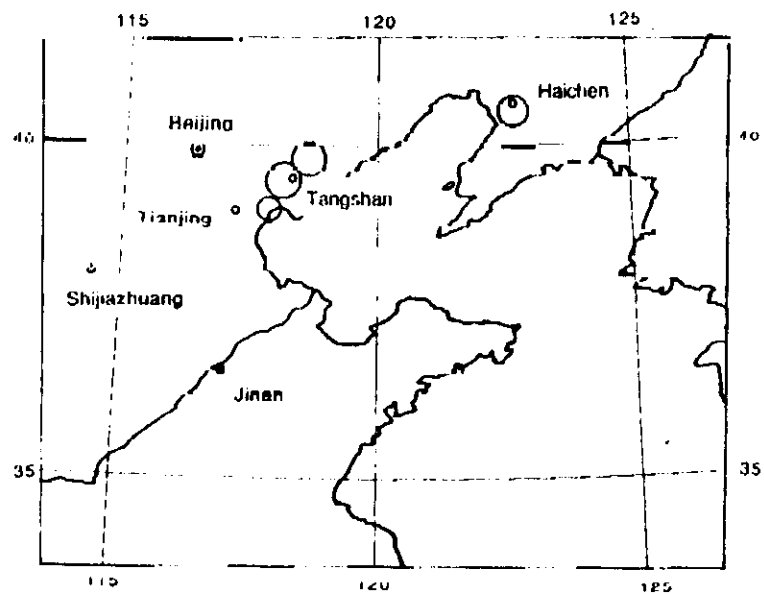


Figure 4